Finite Volume Method as the Numerical Method for New Emulsion Polymerization Tubular Reactor with Internal Angle Baffles

Florentino L. Mendoza Marín,[1] Liliane Maria Ferrareso Lona,[2] Maria R. Wolf Maciel,[1] Rubens Maciel Filho[1]

[1]*Laboratory of Optimization, Design and Advanced Process Control (LOPCA), Faculty of Chemical Engineering, State University of Campinas (UNICAMP), Campinas, SP, Brazil*
[2]*Laboratory of Analysis and Simulation of Chemical Process, Department of Chemical Processes, Faculty of Chemical Engineering, State University of Campinas (UNICAMP), Campinas, SP, Brazil*

Received 21 January 2006; accepted 25 July 2006
DOI 10.1002/app.25215
Published online in Wiley InterScience (www.interscience.wiley.com).

ABSTRACT: A finite volume method is used to solve a determinist mathematical model and to analyze the performance of an alternative design for an emulsion polymerization reactor with internal angular baffles as static mixer. It is assumed to be a steady-state, cylindrical one-dimensional model having a fully developed laminar plug flow. The Smith-Ewart model is used to estimate the monomer conversion, the kinetics is of Arrhenius type, and laminar finite-rate model is assumed to compute chemical source terms. The objective of this work is to develop the finite volume method for the new emulsion polymerization tubular reactor with internal angle baffles. The performance of the alternative reactor is compared with continuous tubular reactor with constant reaction temperature. The simulations were validated with experimental results for the isothermal and tubular reactor, with a good concordance. The results with baffles were better than without baffles in relation to desired properties such as particle size and viscosity. The problem is sufficiently well solved by finite volume method.
 J Appl Polym Sci 102: 6037–6048, 2006

Key words: modeling; simulation; emulsion; polymerization; finite volume methods; baffled tubular reactor

INTRODUCTION

Finite volume method deals with equations from conservative balance in a finite control volume, taking into account variables and parameter distributions in agreement with Gauss' divergence theorem, used as a finite volume condition at the domain and subdomain like boundary conditions. Moreover, it can be used to estimate the variable profiles and material properties by means of computationally algebraic solutions.[1] This is a powerful solution procedure to investigate, through simulation, the behavior and performance of processes and equipment.

The fundamentals of emulsion polymerization are now sufficiently well understood that new products can be made, and old ones reformulated in new ways that can lead to significant improvements in performance and production characteristics. The emulsion polymerization is economically important: for example, current production of all polymers is more than 10^8 tons per year, and ~30% of this polymer is made by free-radical means; emulsion methods are used for effecting 40–50% of these free-radical polymerizations. It is a heterogeneous reaction process in which unsaturated monomers are dispersed in a continuous phase with the aid of an emulsifier system and polymerized with free-radical initiators. It leads to a high molecular weight polymer and high reaction rates in many cases. It has low viscosity, which is a specific advantage when compared with other polymerization techniques.[2–5] Emulsion polymerization is a complex heterogeneous process involving transport of monomer, free radicals, and other species between aqueous and organic phases. It is compared to other heterogeneous polymerizations, like suspension or precipitation, but it is likely the most complicated system; all these factors make modeling of this system very difficult.[6,7]

The chemical processes in the chemical industry have growing operational difficulties caused by the diversification and specification of products, and investigations for alternative reactor design and analysis of their behavior under static and dynamic conditions are welcome. In tubular reactor (TR) most reaction happens towards the reactor entrance, and the variable reaction temperature for exothermic reactions

Correspondence to: F. L. Mendoza Marín (marin@lopca.feq.unicamp.br) or R. Maciel Filho (maciel@feq.unicamp.br).
Contract grant sponsor: The PEC-PG/CAPES.

as well as the limitations to heat transfer near the wall make the behavior very complex.[8–10]

The emulsion polymerization reaction is exothermic ($\Delta H = -16.7$ kcal/mol), and the effect of polymerization in fluid viscosity as well as its impact on the heat transfer limitations call for a need to investigate alternative reactor design. In fact, conventional TR may have serious limitations to heat transfer, leading to products with undesired conditions. Bearing this in mind, in this work an alternative TR based on the placement of baffles inside the reactor is proposed. The objective of this work is to model, simulate, and analyze the emulsion polymerization reactor performance, and develop a solution procedure based on finite volume method for the new emulsion polymerization TR with internal angle baffles. Also, it is compared with continuous TR with constant reaction temperature.

REACTIONAL SYSTEM

Conditions of test

To evaluate the performance of the proposed design, the emulsion polymerization of styrene (EPS) is considered and comparison with conventional TR is carried out. Figure 1 shows the proposed alternative reactor. To represent the system, a simplified one-dimensional deterministic model is developed with the following assumptions: flow along the axial direction (negligible diffusion); fully developed axial velocity of fluid flow; polymer particle phase is the main locus of polymerization. Also the monomer conversion is estimated by Smith-Ewart model, the kinetics is of Arrhenius type, and laminar finite-rate model is assumed to compute chemical source. The finite volume method is used to solve the one-dimensional deterministic model.

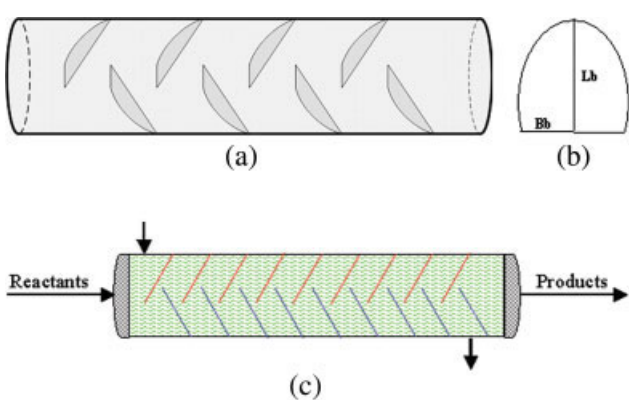

Figure 1 (a) Schematic representation of polymerization TR with baffles. (b) Area of baffle. Bb is the base of baffle, and Lb is the length of each baffle. (c) Profile of polymerization TR with internal-inclined angular baffles. [Color figure (subpart c) can be viewed in the online issue, which is available at www.interscience.wiley.com.]

Properties

To evaluate the performance of the proposed alternative reactor design, the EPS was considered, specifically the work of Bataile.[11] The homopolymerization emulsion of styrene is carried out at 60°C with the concentration of 0.026 mol of potassium persulfate (KPS)/L, 0.070 mol of sodium dodecyl sulfate (SDS)/L, 8.39 mol of styrene/L, and 161.52 mol of water/L in the emulsion. Table I resumes the main system information, and more detail can be found in Mendoza Marín.[12]

MATHEMATICAL MODELING

To represent the proposed reactor shown in Figure 1, with the case study of emulsion homopolymerization of styrene, the following model equation may be written.

Chemical reaction

The mechanism of EPS may be schematically and briefly shown as

$$\text{Initiation}: \mathrm{I_2} \xrightarrow{K_d} 2\mathrm{I}^- \quad \mathrm{I}^- + \mathrm{M} \xrightarrow{K_p} \mathrm{R_1} \tag{1}$$

where I_2 is the initiator, I^- is the primary radicals from initiator, M is the monomer concentration, and R_1 is the radical or oligomeric radical with chain length 1.

Radical absorption by micelle surface (micellar nucleation (MN)):

$$\begin{gathered}\text{Diffusion in the water phase} \\ R_{\mathrm{rw}} \xrightarrow{K_{\mathrm{cmw}}} R_{\mathrm{rw}}\mathrm{MIC} \\ \text{Absorption in the micelle surface} \\ R_r + \mathrm{MIC} \overset{K_{\mathrm{cm}}:K_{\mathrm{cmd}}}{\longleftrightarrow} R_r\mathrm{MIC}\end{gathered} \tag{2}$$

Radical absorption by particles surface (homogeneous nucleation (HN)):

$$\begin{gathered}\text{Diffusion in the water phase} \\ R_{\mathrm{rw}} \xrightarrow{K_{\mathrm{cpw}}} R_{\mathrm{rw}}\mathrm{PP} \\ \text{Absorption in the particle surface} \\ R_r + \mathrm{PP} \overset{K_{\mathrm{cp}}:K_{\mathrm{cpd}}}{\longleftrightarrow} R_r\mathrm{PP}\end{gathered} \tag{3}$$

$$\text{Propagation}: R_r + \mathrm{M} \xrightarrow{K_p} R_{r+1} \tag{4}$$

Termination: by combination (Ktc) and disproportionation (Ktd)

$$R_n + R_m \xrightarrow{K_{\mathrm{tc}}} P_{n+m} \quad \text{or} \quad R_n + R_m \xrightarrow{K_{\mathrm{td}}} P_n + P_m \tag{5}$$

TABLE I
Main System Properties of Styrene as Database for Simulation of EPS, Including Grid, Particles, Reactor, and Baffles Data

Symbol	Value (unit) [description]
Na	6.02×10^{23} (molecule/mol) [Avogadro's number: $\pi = 3.14159$]
R_g	1.987 (cal/mol K) [gas constant]
ρ_p, ρ_m	$1.25 - 0.0004202T$ (kg/L) [polymer density] and $0.949 - 0.00128\ (T - 273.15)$ (kg/L) [monomer density]
anrp	0.5 [average number of radicals per particle]
CMC	0.008 (mol/L) [critical micelle concentration]
CMw	0.005 (mol/L) [monomer concentration in water phase ($=M_w$)]
f_i	0.5 [initiator efficiency]
K_{cm}	$4\pi Dwr_{mic}N_A$ (min^{-1}) [rate const of aqueous phase radical capture by micelles
K_{cp}	$4\pi Dpr_pN_A$ (min^{-1}) [rate const of radical capture by polymer particles
K_d	$1.524 \times 10^{18} \exp(-33320/R_gT)$ (min^{-1}) rate const of initiator decomposition
K_p	$4.703 \times 10^{11} \exp(-9805/RgT)$ (L/mol min); rate const of propag. of poly. partis
K_t	$1.04619 \times 10^{10} \exp(-2950.45/RgT)$ (L/mol min) [global rate const for termination]
$[M]_P$	$(1 - \phi_p)\rho_m/MWs$ (mol/L) [monomer concentration in polymer particle]
MW_e	288.38 (g/mol) [molecular weight of surfactant]
MW*i*	271.3 (g/mol) [molecular weight of initiator]
MW*s*	104 (g/mol) [molecular weight of styrene]
Ncr	5 [critical chain length at which water phase radical can be absorbed]
n_{em}	60 (no. emul/mic) [number of emulsifier molecules in a micelle]
Sa	3×10^{-17} (dm^2) [area covered by one molecule of emulsifier]
ϕ_p, ϕ_m	0.4 [volume fraction of polymer]; 0.6 [volume fraction of monomer]
Re	5000 (laminar) and 13,600 (turbulent) [Reynolds number]
v_{in}	0.27027 (laminar) and 0.7351 (turbulent) (m/min) [inlet velocity in TR]
D_p	1.76×10^{-12} (dm^2/min) [diffusivity of monomer radicals in polymer phase]
D_w	1.76×10^{-9} (dm^2/min) [diffusivity of monomer radicals in water phase]
μ	0.001 (Kg/m s) [viscosity of polymer]
T_{in}	333.15 and 363.15 (K) [inlet temperatures to the reactor]
ΔH	−16682.2 (cal/mol) [polymerization reaction heat of styrene]
N	51 [number of nodal points]
r_{mic}, r_p	27.5 (Å) [radius of micelle] and 275 (Å) [radius of polymer]
D_r, L_r	1 (m) [diameter of TR] and 20 (m) [length of TR]
L_{br}	1 (m) [length of baffle separation] and $N_b = 6$, 18 [number of baffles]

Conservative models

Principle of mass conservation in general form for a chemical species j reacting in a flowing fluid with varying density, temperature, and composition is

$$\frac{\partial C_j}{\partial t} + \nabla \cdot \left(C_j \vec{u}\right) + \nabla \cdot J_j = R_j \tag{6}$$

where C_j is the molar concentration of species j; $\partial C_j/\partial t$ is the no steady-state term expressing accumulation or depletion; $\bigtriangledown$ is the gradient operator; $\nabla \cdot \vec{u}$ is the divergence of a vector function $\vec{u}$; $\vec{u}$ is the three-dimensional mass-average velocity vector; $\nabla \cdot (C_j\vec{u})$ is the transport of mass by convective flow; J_j is the molar flux vector for species j with respect to the mass-average velocity; $\bigtriangledown \cdot JM_j$ is molecular diffusion only; R_j is the total rate of change of the amount of j because of reaction. Species j occurs in liquid phase. The equation can be taken for single-phase or ''homogeneous'' or ''pseudo homogeneous'' reactors.[13]

The generalized *laminar finite-rate model* was applied to compute the chemical source terms (R_j). The model is exact for laminar flow, but is generally inaccurate for turbulent require because of highly nonlinear chemical kinetics of Arrhenius type. The net source of chemical species j due to reaction R_j is computed as the sum of the Arrhenius reaction sources over the N_i reactions that the species participate in:

$$R_j = \sum_{i=1}^{N_i} R_{j,i} = \sum_{i=1}^{N_i} \left(K_{f,i} \prod_{i=1}^{N_i} [C_{j,i}]^{n_{fj,i}} - K_{b,i} \prod_{i=1}^{N_i} [C_{j,i}]^{n_{bj,i}} \right) \tag{7}$$

where $R_{j,i}$ is the Arrhenius molar rate of creation/destruction of species j in reaction i; $K_{f,i}$ is the forward rate constant for reaction i, $K_{b,i}$ is the backward rate constant for reaction i, N_i is the number of chemical species in reaction i, $C_{j,i}$ is the molar concentration of each reactant and product species j in reaction i, $n_{fj,i}$ is the forward rate exponent for each reactant and product species j in reaction i, $n_{bj,i}$ is the backward rate exponent for each reactant and product species j in reaction i. Only nonreversible reactions were considered, and the mass balance of equations gives the different chemical source term as free radical (R_{Rw}), ini-

tiator (R_I), monomer (R_M), surfactant ($R_E = 0$, by to be inert in EPS), and polymer (R_P):

$$R_{RW} = R_I - R_I\left[\frac{K_pM_w}{K_pM_w + K_{cp}[N_P] + K_{tw}[R]_w}\right]^{ncr-1} - K_{cp}[N_P] \times [R]_w - K_{cm}[MIC][R]_w - K_{tw}[R]_w^2 \quad (8)$$

$$R_I = -fiK_d[I]_w(8) \quad (9)$$

$$R_M = -\frac{K_p[M]_P N_P \overline{n}}{N_A V_P} - K_{pw}[M]_w[R]_w \quad (10)$$

$$R_P = \frac{K_p[M]_P N_P \overline{n}}{N_A V_P} + K_{pw}[M]_w[R]_w \quad (11)$$

Newton's second law of momentum was applied to a small volume element moving with the fluid that is accelerated because of the forces acting over it. The motion equation in terms of τ is

$$\rho\frac{D\vec{u}}{Dt} = -\nabla P + (\nabla \cdot \vec{\tau})\rho \cdot \vec{g} \quad (12)$$

Here $\vec{g}$ represents the body forces per unit area; ρ is the density; P is the pressure; $\vec{\tau}$ is the extra stress tensor, and D/Dt is the material or substantial derivative.[14,15]

In the *micellar nucleation* (MN), it is accepted that particles are generated by micelle absorbing radicals from the water phase[1]:

The rate of particle formation by micellar nucleation (R_{MN}) (see mechanism) is given by

$$R_{MN} = \frac{d[N_p]_m}{dt} = K_{cm}[MIC] \times [R]_w \quad (13)$$

The formation rate of total oligomeric radicals in the aqueous phase ($[R]_w$) was obtained by the mechanism of emulsion polymerization and the steady-state hypothesis approximations, and the geometric progression approximations[4,7,12] were applied so that

$$[R]_w = \frac{R_I}{K_pM_w + K_{cm}[MIC] + K_{tw}[R]_w}\left(\frac{1-\alpha_m^{ncr-1}}{1-\alpha_m}\right) \quad (14)$$

The probability of the oligomeric radical dead to micelle propagation (α_m) is as

$$\alpha_m = \frac{K_pM_w}{K_pM_w + K_{cm}[MIC] + K_{tw}[R]_w + K_{cp}[N_p]} \quad (15)$$

In the *homogeneous nucleation* (HN), it is accepted that the particles could be generated by precipitated water phase oligomeric radicals, and the rate of particle formation by homogeneous nucleation (R_{HN}) (see Mechanism) can be written as[1]

$$R_{HN} = \frac{d[N_p]_h}{dt} = K_pM_w[R_{ncr-1}]_w \quad (16)$$

For the formation rate of oligomeric radicals with critical chain length (ncr) in the aqueous phase ($[R_{ncr-1}]_w$) the same hypothesis adopted for $[R]_w$ was considered.

$$[R_{ncr-1}]_w = \frac{R_I}{K_pM_w}\alpha_h^{ncr-1} \quad (17)$$

The probability of an oligomeric radical dead to lead to a homogeneous propagation (α_h) is given by

$$\alpha_h = \frac{K_pM_w}{K_pM_w + K_{tw}[R]_w + K_{cp}[N_p]} \quad (18)$$

Characterization of polymer particle

The polymer particle (by MN and HN) is determined with eq. (6) written like eq. (19) and source term as eq. (20):

$$\frac{\partial C_{N_P}}{\partial t} + \left(v_r\frac{\partial C_{N_P}}{\partial r} + v_\theta\frac{1}{r}\frac{\partial C_{N_P}}{\partial \theta} + v_z\frac{\partial C_{N_P}}{\partial z}\right) = D_{NB}\left(\frac{1}{r}\frac{\partial}{\partial r}\left(r\frac{\partial C_{N_P}}{\partial r}\right) + \frac{1}{r^2}\frac{\partial^2 C_{N_P}}{\partial \theta^2} + \frac{\partial^2 C_{N_P}}{\partial z^2}\right) + R_{N_P} \quad (19)$$

$$R_{N_p} = R_{MN} + R_{HN} = \frac{K_{cm}[MIC]R_I}{K_pM_w + K_{cm}[MIC] + K_{tw}[R]_w}\left(\frac{1-\alpha_m^{ncr-1}}{1-\alpha_m}\right) + R_I\alpha_h^{ncr-1} \quad (20)$$

The *molecular weight distribution* is determined through the mechanism of EPS. Moments of molecular weigh distribution, coupled with techniques to solve the equations, allow to solve the polymerization reaction. The kinetic solution includes direct sequential solution, discrete transformation method, and moments method. The discrete transformation method includes the steps of chemical reaction, kinetic equation, integration, expansion in power series, drop operator, and applied moments. The kinetic equation is solved through the generating function. The *cumulative dead polymer* was given through

the number-average molecular weight (M_n^c) and weight-average molecular weight (M_w^c):

$$M_n^c = \frac{2a\mathrm{MW}_s}{a-b}\frac{X_j}{\ln\left(\frac{b-aX_j}{b}\right)}$$

$$M_w^c = \mathrm{MW}_s\left(\frac{a+2b}{b-a} - \frac{3a}{2(b-a)}X_j\right) \quad (21)$$

$$\text{where } a = K_p[\mathrm{M}] \quad b = a + K_{\mathrm{tc}}[R]_w \quad (22)$$

The average swollen (R_s) and unswollen (R) *particle polymer size* radius[16] are

$$R_s = \left(\frac{3}{4\pi\rho_P\phi_P}\frac{\mathrm{MW}_p C_{Ps}}{N_A C_{N_P}}\right)^{1/3}$$

$$R = R_s\left(\frac{\rho_m}{\rho_m + [\mathrm{M}]_p\mathrm{MW}_m}\right)^{-1/3} \quad (23)$$

The viscosity of polymer (μ) was estimated[17] as

$$\ln(\mu) = -13.04 + \frac{2013}{T} + \mathrm{MW}_P^{0.18}\left[3.915X_j - 5.437X_j^2 + \left(0.623 + \frac{1387}{T}\right)X_j^3\right] \quad (24)$$

*R*eactor and baffle: Geometry effect

The *internal transversal areas over or beneath baffles* were calculated through geometric equations. In such equations, α is the increment angle from the TR center point until total diameter (αr is in rad), θ is the increment angle to calculate the fluid flow area of EPS beneath or over the baffles (θr is in rad), A_{vb} is fluid flow variable area inside TR beneath or over baffles, A_r is the area of TR without baffles [Fig. 2(a)], and A_{fb} is the fixed area inside TR over or beneath baffles. Figure 2 shows the variation of the transversal area available to the reactant flow inside the reactor.

$$\alpha r(1) = \arcsin\left(2\frac{ID(1)}{D_r}\right) \quad (25)$$

$$\theta r(1) = \frac{\pi}{180}\theta g(1) = \pi\left(1 - 2\frac{\alpha r(1)}{\pi}\right) \quad (26)$$

$$A_{\mathrm{vb}}(1) = \frac{{D_r}^2}{8}(\theta r(1) - \sin\theta r(1)) \quad (27)$$

$$A_{\mathrm{fb}}(1) = A_r - A_{\mathrm{vb}}(1) = \frac{\pi}{4}D_r^2 - A_{\mathrm{vb}}(1) \quad (28)$$

Calculus of A_{vb} from I = 2 to number of areas beneath or over baffles (N_{ab}) [see Fig. 2(b–f)]

$$D_{\mathrm{vb}}(I) = D_{\mathrm{vb}}(I-1) + \Delta D_{\mathrm{vb}} \quad (29)$$

$$\alpha r(I) = \arcsin\left(2\frac{\mathrm{ID}(I)}{D_r}\right) = \arcsin\left(\frac{2}{D_r}(D_{\mathrm{vb}}(I) - 0.5^* D_r)\right) \quad (30)$$

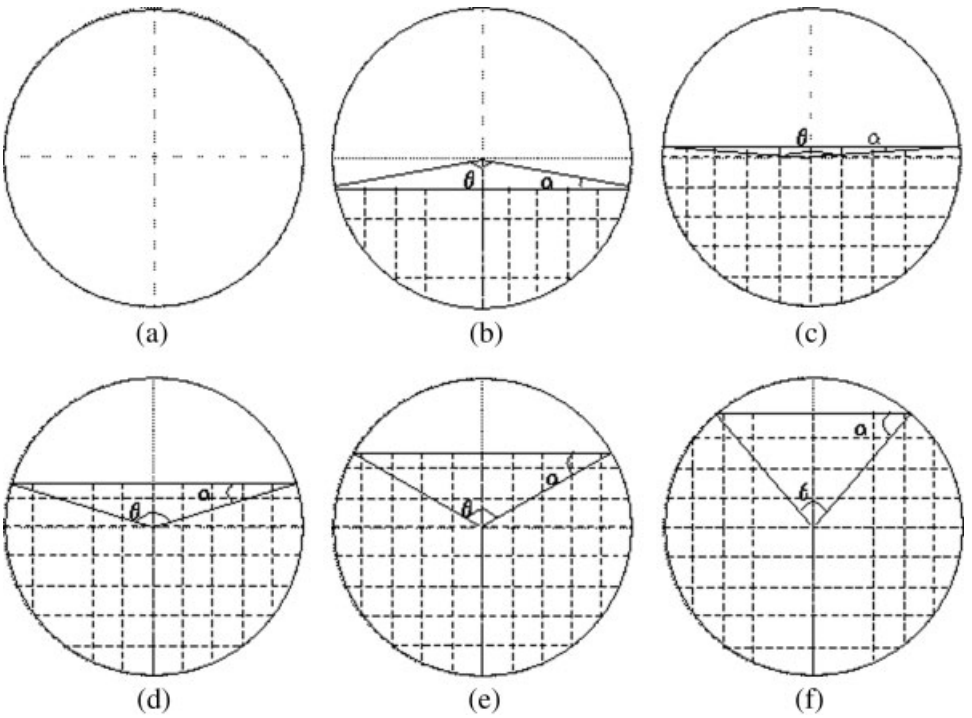

Figure 2 Variation of transversal area of fluid flow of EPS inside TR beneath or over baffles.

$$\theta r(I) = \frac{\pi}{180}\theta g(I) = \pi\left(1 - \frac{2}{\pi}\alpha r(I)\right) \tag{31}$$

$$A_{\mathrm{fb}}(I) = \frac{{D_r}^2}{8}(\theta r(I) - \sin\theta r(I)) \tag{32}$$

$$A_{\mathrm{vb}}(I) = A_r - A_{\mathrm{fb}}(I) \tag{33}$$

where ID is the interval of increment of diameter from the point of fixed diameter until total diameter, and D_{vb} is the variable diameter of fluid flow in tubular reactor beneath or over baffles.

The *internal transversal areas inside TR without and with baffles* (A_z) are presented in this work as an example only for $N = 50$ finite volume and $N_b = 18$ baffles [see Fig. 2(a–f)].

Area at the TR inlet

$$A_z(1) = A_r \tag{34}$$

$$A_z(2) = A_r \tag{35}$$

$$A_z(3) = A_r \tag{36}$$

Area at the internal TR from I = 4 to $N-3$, with step of 5

$$A_z(I) = A_{\mathrm{vb}}(1) \tag{37}$$

$$A_z(I+1) = A_{\mathrm{vb}}(3) \tag{38}$$

$$A_z(I+2) = A_{\mathrm{vb}}(5) \tag{39}$$

$$A_z(I+3) = A_{\mathrm{vb}}(2) \tag{40}$$

$$A_z(I+4) = A_{\mathrm{vb}}(4) \tag{41}$$

Area at the TR outlet from I = $N-2$ to N

$$A_z(N-2) = A_r \tag{42}$$

$$A_z(N-1) = A_r \tag{43}$$

$$A_z(N) = A_r \tag{44}$$

The *axial velocity* at TR inlet over or beneath baffles and temperature effects were estimated from Newton's second law of momentum and continuity equation. In the equations, v_{in} is the axial velocity at TR inlet in isothermal condition (see Table I), and v_b is the axial velocity over or beneath baffles in isothermal condition [see Fig. 2(a–f)].

$$v_{\mathrm{in}} = \frac{\mu R_e}{\rho D_r} \qquad v_b = \frac{\mu A_r R_e}{\rho A_{\mathrm{vb}} D_r} \tag{45}$$

The *axial velocity inside TR without and with baffles* (v_z) were calculated in this work as an example only for $N = 50$ finite volumes and $N_{\mathrm{b}} = 18$ baffles [see Fig. 2(a–f)].

The reactant velocities at the TR inlet are given by

$$v_z(1) = v_{\mathrm{in}} \tag{46}$$

$$v_z(2) = v_{\mathrm{in}} \tag{47}$$

$$v_z(3) = v_{\mathrm{in}} \tag{48}$$

Velocities at the internal TR from I = 4 to $N-3$, with step of 5

$$v_z(\mathrm{I}) = v_b(1) \tag{49}$$

$$v_z(\mathrm{I}+1) = v_b(3) \tag{50}$$

$$v_z(\mathrm{I}+2) = v_b(5) \tag{51}$$

$$v_z(\mathrm{I}+3) = v_b(2) \tag{52}$$

$$v_z(\mathrm{I}+4) = v_b(4) \tag{53}$$

Velocities at the TR outlet from I = $N-2$ to N

$$v_z(N-2) = v_{\mathrm{in}} \tag{54}$$

$$v_z(N-1) = v_{\mathrm{in}} \tag{55}$$

$$v_z(N) = v_{\mathrm{in}} \tag{56}$$

NUMERICAL METHOD

The most usual numerical methods used to solve a large class of engineering problems are finite difference, finite elements, orthogonal collocation, and boundary elements method, which can solve ordinary or partial equations by means of approximations, according to particular problem and finalities.[12]

In this work, finite volume method was used as the numerical method according to Versteeg, Malalasekara, and Patankar.[15,18] For the finite volume method implementations were used following the procedure: the general transport equations can be written in differential form; grid generation can be written for all discrete control volume, discretization of general transport equations and solution of algebraic equations and tests of convergence for the numerical method.[12] The *discrete approximation* was applied to the conservative balance of convection and source only, e.g., the equation of particle number, eq. (19) and source term or the overall rate of formation of particles by MN and HN [eq. (20)].

Linear approximation

The discretization is calculated for a number of particles. It can be expanded for scalar variables such as concentration, velocity, and temperature. The con-

servative balance for discrete approximation is the eq. (6) written as eq. (19) in one-dimensional domain. The *linear approximation* was applied to source term of eq. (20). The Taylor's series method of linearization was used to linearize S_ϕ. The overall equation of source-term linearization, ($S_\phi = S_{N_p}$) in eq. (20) leads to

$$S_{N_p} = R_{N_p} = R_{\mathrm{MN}} + R_{\mathrm{HN}} = S_{N_{\mathrm{pm}}} + S_{N_{\mathrm{ph}}} = \mathrm{SUT} - \mathrm{SPT}[N_p]_{\mathrm{P}} \quad (57)$$

where SUT is all linear coefficients, SPT is all angular coefficients, $[N_p]_P$ is the concentration of number of particles in the nodal point P (control volume).

The source-term linearization for *micellar nucleation* ($R_{\mathrm{MN}} = S_{N_{pm}}$) is written [see eq. (57)] as

$$S_{N_{\mathrm{pm}}} = R_{\mathrm{MN}} = \mathrm{SUM} - \mathrm{SPM}[N_p]_P \quad (58)$$

where SUM is the micellar linear coefficient, and SPT is the micellar angular coefficient.

Equation (13) can be rewritten as given in eq. (59), and the notation of nodal point P will be omitted.

$$S_{N_{\mathrm{pm}}} = R_{\mathrm{MN}} = m4\left(\frac{m3 + K_{\mathrm{cp}}[N_p]}{m2 + k_{\mathrm{cp}}[N_p]}\right)\left(1 - \left(\frac{m1}{m3 + K_{\mathrm{cp}}[N_p]}\right)^{\mathrm{ncr}-1}\right) \quad (59)$$

Taylor's series for one variable was applied to linearize the source-term, eq. (59) which is a polynomial approximation of degree $n = 1$. The linearization represents the tangent to the $S_{\mathrm{N_{pm}}} - [N_p]_P$ curve at $[N_{\mathrm{pa}}]$.

$$S_{N_{\mathrm{pm}}}([N_p]) = S_{N_{\mathrm{pm}}}([N_{\mathrm{pa}}]) + S'_{N_{\mathrm{pm}}}([N_{\mathrm{pa}}])([N_p] - [N_{\mathrm{pa}}]) \quad (60)$$

where

$$S_{N_{\mathrm{pm}}}([N_{\mathrm{pa}}]) = m4\left(\frac{m3 + K_{\mathrm{cp}}[N_{\mathrm{pa}}]}{m2 + K_{\mathrm{cp}}[N_{\mathrm{pa}}]}\right) \times \left(1 - \left(\frac{m1}{m3 + K_{\mathrm{cp}}[N_{\mathrm{pa}}]}\right)^{\mathrm{ncr}-1}\right) \quad (61)$$

$$S'_{N_{\mathrm{pm}}}([N_{\mathrm{pa}}]) = \left(\frac{(\mathrm{ncr}-1)m4K_{\mathrm{cp}}}{m2 + K_{\mathrm{cp}}[N_{\mathrm{pa}}]}\right)\left(\frac{m1}{m3 + K_{\mathrm{cp}}[N_{\mathrm{pa}}]}\right)^{\mathrm{ncr}-1} - \left(\frac{m1m4K_{\mathrm{cp}}}{(m2 + K_{\mathrm{cp}}[N_{\mathrm{pa}}])^2}\right)\left(1 - \left(\frac{m1}{m3 + K_{\mathrm{cp}}[N_{\mathrm{pa}}]}\right)^{\mathrm{ncr}-1}\right) \quad (62)$$

$[N_{\mathrm{pa}}]$ is one point of the line tangent [eq. (58)] to the curve $S_{N_{\mathrm{pm}}} = f([N_{\mathrm{P}}])$ [eq. (59)]. This point can be estimated by the following ways:

1. The average value of the intersection points in the coordinate axis of the line tangent [eq. (58)] to the curve [eq. (59)]. The intersection points must be the maximum values in each interception. Whether a curve is concave up or concave down, the value of $[N_{\mathrm{pa}}]$ must be adjusted with care.
2. The average value of the variable $\phi = [N_{\mathrm{p}}]$ of the experimental conditions at TR inlet and outlet.

The following definitions are used to simplify the coefficient SUM of eq. (58):

$$\mathrm{SUM} = \mathrm{SUM1} + \mathrm{SUM2} - \mathrm{SUM3} \quad (63)$$

$$\mathrm{SUM1} = m4\left(\frac{m3 + K_{\mathrm{cp}}[N_{\mathrm{pa}}]}{m2 + K_{\mathrm{cp}}[N_{\mathrm{pa}}]}\right) \times \left(1 - \left(\frac{m1}{m3 + K_{\mathrm{cp}}[N_{\mathrm{pa}}]}\right)^{\mathrm{ncr}-1}\right) \quad (64)$$

$$\mathrm{SUM2} = \left(\frac{m1m4K_{\mathrm{cp}}[N_{\mathrm{pa}}]}{(m2 + K_{\mathrm{cp}}[N_{\mathrm{pa}}])^2}\right) \times \left(1 - \left(\frac{m1}{m3 + K_{\mathrm{cp}}[N_{\mathrm{pa}}]}\right)^{\mathrm{ncr}-1}\right) \quad (65)$$

$$\mathrm{SUM3} = \left(\frac{(\mathrm{ncr}-1)m4K_{\mathrm{cp}}[N_{\mathrm{pa}}]}{m2 + K_{\mathrm{cp}}[N_{\mathrm{pa}}]}\right) \times \left(\frac{m1}{m3 + K_{\mathrm{cp}}[N_{\mathrm{pa}}]}\right)^{\mathrm{ncr}-1} \quad (66)$$

where

$$m1 = K_P M_w, m2 - K_{\mathrm{cm}}[\mathrm{MIC}] + K_{\mathrm{tw}}[R]_w, \quad m3 = m1 + m2, m4 = \frac{K_{\mathrm{cm}}[\mathrm{MIC}]R_I}{m3} \quad (67)$$

To simplify the coefficient SPM of eq. (58), the following definitions are used:

$$\mathrm{SPM} = \mathrm{SPM1} - \mathrm{SPM2} \quad (68)$$

$$\mathrm{SPM1} = \left(\frac{m1m4K_{\mathrm{cp}}}{(m2 + K_{\mathrm{cp}}[N_{\mathrm{pa}}])^2}\right) \times \left(1 - \left(\frac{m1}{m3 + K_{\mathrm{cp}}[N_{\mathrm{pa}}]}\right)^{\mathrm{ncr}-1}\right) \quad (69)$$

$$\mathrm{SPM2} = \left(\frac{(\mathrm{ncr}-1)m4K_{\mathrm{cp}}}{m2 + K_{\mathrm{cp}}[N_{\mathrm{pa}}]}\right)\left(\frac{m1}{m3 + K_{\mathrm{cp}}[N_{\mathrm{pa}}]}\right)^{\mathrm{ncr}-1} \quad (70)$$

Source-term linearization for *homogeneous nucleation* ($R_{\mathrm{HN}} = S_{N_{\mathrm{ph}}}$) is written [see eq. (57)] as

$$S_{N_{\mathrm{ph}}} = R_{\mathrm{HN}} = \mathrm{SUH} - \mathrm{SPH}[N_p]_{\mathrm{P}} \quad (71)$$

where SUH is homogeneous linear coefficient, and SPH is the homogeneous angular coefficient.

Equation (16) can be rewritten as given in eq. (72), and the notation of nodal point P will be omitted.

$$S_{N_{\mathrm{ph}}} = R_{\mathrm{HN}} - R_I \left(\frac{K_p M_w}{K_p M_w + K_{\mathrm{tw}}[R]_w + K_{\mathrm{cp}}[N_p]} \right)^{\mathrm{ncr}-1} \tag{72}$$

Taylor's series for one variable was applied to linearize the source-term, eq. (72) which is polynomial approximation of degree $n = 1$. The linearization represents the tangent to the $S_{N_{ph}} - [N_P]_P$ curve at $[N_{pa}]$.

$$S_{N_{\mathrm{ph}}}([N_p]) = S_{N_{\mathrm{ph}}}([N_{\mathrm{pa}}]) + S'_{N_{\mathrm{ph}}}([N_{\mathrm{pa}}])([N_p] - [N_{\mathrm{pa}}]) \tag{73}$$

where

$$S_{N_{\mathrm{ph}}}([N_{\mathrm{pa}}]) = R_I \left(\frac{h1}{h2 + K_{\mathrm{cp}}[N_{\mathrm{pa}}]} \right)^{\mathrm{ncr}-1} \tag{74}$$

$$S'_{N_{\mathrm{ph}}}([N_{\mathrm{pa}}]) = \frac{(\mathrm{ncr}-1) K_{\mathrm{cp}} R_I h1^{\mathrm{ncr}-1}}{(h2 + K_{\mathrm{cp}}[N_{\mathrm{pa}}])^{\mathrm{ncr}}} \tag{75}$$

$[N_{pa}]$ is one point of the line tangent [eq. (71)] to the curve $S_{N_{pm}} = f([N_P])$ [eq. (72)]. This point can be estimated by the following ways:

1. The average value of the intersection points in the coordinate axis of the line tangent [eq. (71)] to the curve [eq. (72)]. The intersection points must be maximum values in each interception. Care has to be taken in relation to the adjustment of the $[N_{pa}]$ values whether the curve may be concave up or concave down.
2. The average value of the variable $\phi = [N_P]$ of the experimental conditions at TR inlet and outlet.

The value $[N_{pa}]$ estimated by homogeneous nucleation was used for source-term linearization by micellar nucleation.

The following definitions are used to simplify the linear coefficient SUH of eq. (71):

$$\mathrm{SUH} = \mathrm{SUH1} + \mathrm{SUH2} \tag{76}$$

$$\mathrm{SUH1} = R_I \left(\frac{h1}{h2 + K_{\mathrm{cp}}[N_{\mathrm{pa}}]} \right)^{\mathrm{ncr}-1} \tag{77}$$

$$\mathrm{SUH2} = \frac{(\mathrm{ncr}-1) K_{\mathrm{cp}} R_I [N_{\mathrm{pa}}]}{h1} \left(\frac{h1}{h2 + K_{\mathrm{cp}}[N_{\mathrm{pa}}]} \right)^{\mathrm{ncr}} \tag{78}$$

where

$$h1 = K_p M_w,\ h2 = h1 + K_{\mathrm{tw}}[R]_w \tag{79}$$

The following definition is used to simplify the angular coefficient SPH of the eq. (71)

$$\mathrm{SPH} = \frac{(\mathrm{ncr}-1) K_{\mathrm{cp}} R_I}{h1} \left(\frac{h1}{h2 + K_{\mathrm{cp}}[N_{\mathrm{pa}}]} \right)^{\mathrm{ncr}} \tag{80}$$

Now the eqs. (63) and (76) are used to obtain the linear coefficient SUT of the eq. (57) through

$$\mathrm{SUT} = \mathrm{SUM} + \mathrm{SUH} \tag{81}$$

and the eqs. (68) and (80) are considered to obtain the angular coefficient SPT of the eq. (57).

$$\mathrm{SPT} = \mathrm{SPM} + \mathrm{SPH} \tag{82}$$

Integration

The integral forms of the general transport equations represent the key step of the finite volume method. The integration of the eqs. (6) or (19) is made over the control volume (cv). The *integral form* of general steady transport equations in one-dimensional control volume without diffusion is given by

$$\int_{\mathrm{cv}} \frac{\partial (v_z N_p)}{\partial z} A\, dz = \int_{\mathrm{cv}} S_{N_p} A\, dz = \int_{\mathrm{cv}} (\mathrm{SUT} - \mathrm{SPT} \times N_{p_p}) A\, dz \tag{83}$$

$$(AvN_p)_e - (AvN_p)_w = (S_{N_p} Az)_e - (S_{N_p} Az)_w = (\mathrm{SUT} - \mathrm{SPT} \times N_{p_p}) A_p\, \Delta z \tag{84}$$

The continuity equation is

$$(Av\rho)_e = (Av\rho)_w \tag{85}$$

Interpolation

Several methods may be used for interpolation as central differencing: the exact solution, the exponential scheme, the hybrid scheme, the power-law scheme, and upwind differencing.[15,18,19] In this work the upwind difference scheme was applied to calculate the particle number as

$$\begin{aligned} F_w \phi_w &= \phi_W \| F_w, 0 \| - \phi_P \| - F_w, 0 \| \\ F_e \phi_e &= \phi_P \| F_e, 0 \| - \phi_E \| - F_e, 0 \| \end{aligned} \tag{86}$$

$$F = \rho v \tag{87}$$

where F is the mass flux, F_w for west side, and F_e for east side.

Mass balance or continuity equation:

$$A_w\|-F_w,0\| = A_w\|F_w,0\| - A_wF_w$$
$$A_e\|-F_e,0\| = A_e\|-F_e,0\| + A_eF_e \quad (88)$$

where A_w is the west side area of the control volume, and A_e is the area for east side of the control volume.

After integration and interpolation, the *linear algebraic equations* are obtained. In the minimum control volume the discretised equation for minimum control volume is

$$a_P N_{p,\mathrm{P}} = a_E N_{p,\mathrm{E}} + S_U \quad (89)$$

where: $a_W = 0, a_{\mathrm{in}} = A_w\|F_w,0\|, a_E = A_e\|-F_e,0\|,$

$$a_P = a_E + S_P \quad (90)$$

$$S_P = \mathrm{SPT} \times A_P\,\Delta z + a_{\mathrm{in}} + (A_eF_e - A_wF_w),$$
$$S_U = \mathrm{SUT} \times A_P\,\Delta z + a_{\mathrm{in}}N_{p,\mathrm{in}} \quad (91)$$

In the internal control volume from I = 3 to I = $N-2$, the discretised equation for internal control volume is

$$a_P N_{p,\mathrm{P}} = a_W N_{pW} + a_E N_{p,\mathrm{E}} + S_U \quad (92)$$

where

where: $a_W = A_w\|F_w,0\|, a_E = A_e\|-F_e,0\|, a_P$

$$= a_W + a_E + S_P \quad (93)$$

$$S_P = \mathrm{SPT} \times A_P\,\Delta z + (A_eF_e - A_wF_w), S_U = \mathrm{SUT} \times A_p\,\Delta z \quad (94)$$

In the maximum control volume I = $N-1$, the discretised equation for maximum control volume is given as

$$a_P N_{p,\mathrm{P}} = a_E N_{p,\mathrm{E}} + S_U \quad (95)$$

where

$$a_W = A_w\|F_w,0\|, a_E = 0, a_P = a_W + S_p \quad (96)$$

$$S_P = \mathrm{SPT} \times A_p\,\Delta z + (A_eF_e - A_wF_w), S_U = \mathrm{SUT} \times A_p\,\Delta z \quad (97)$$

where a_{in}, a_W, a_{P}, a_E are coefficients of discretised equations by inlet, west, central, and east side of control volume; $N_{P_{\mathrm{in}}}$, N_{P_W}, N_{P_P}, N_{P_E} are the number of particles at inlet, west, central, and east side of control volume; S_U and S_P are linear and angular volumetric source term of scalar variable; z is the axial cylindrical coordinate.

The *solution of algebraic equations* as a system of linear algebraic equations was obtained by Thomas Algorithm or the tridiagonal matrix algorithm as direct method for one-dimensional situation prob-

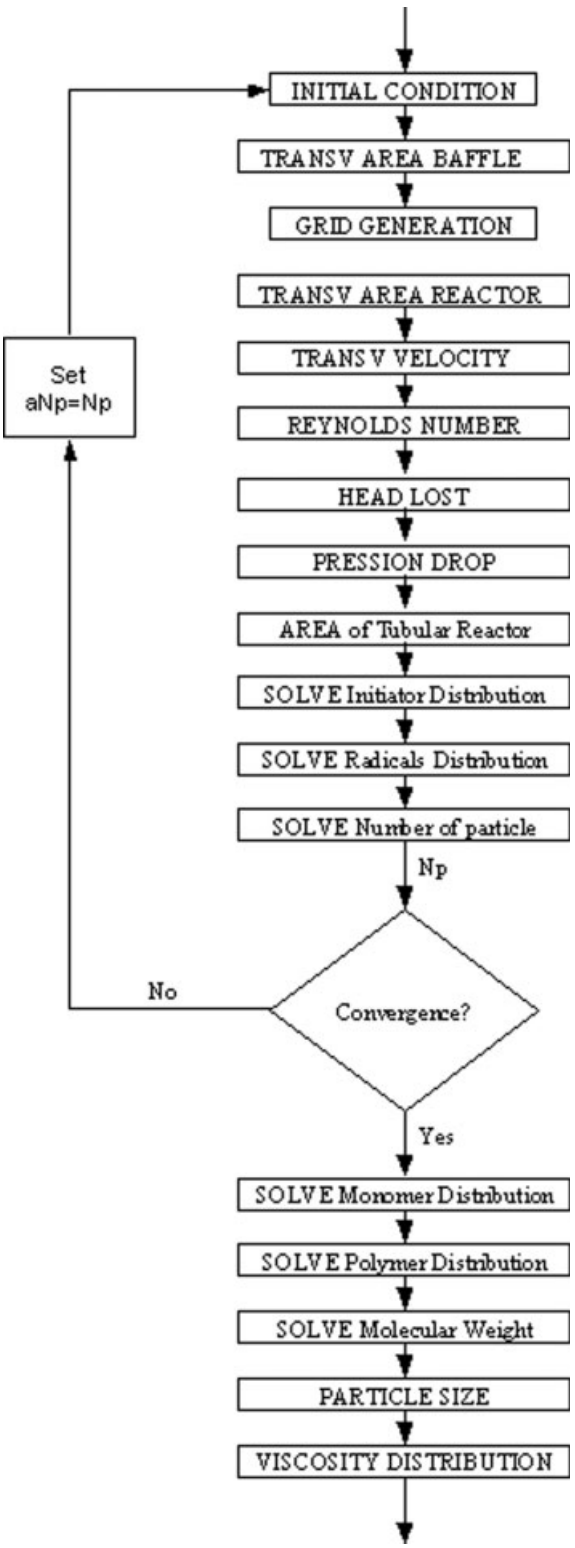

Figure 3 Isothermal condition logic flow diagram with internal angular baffles.

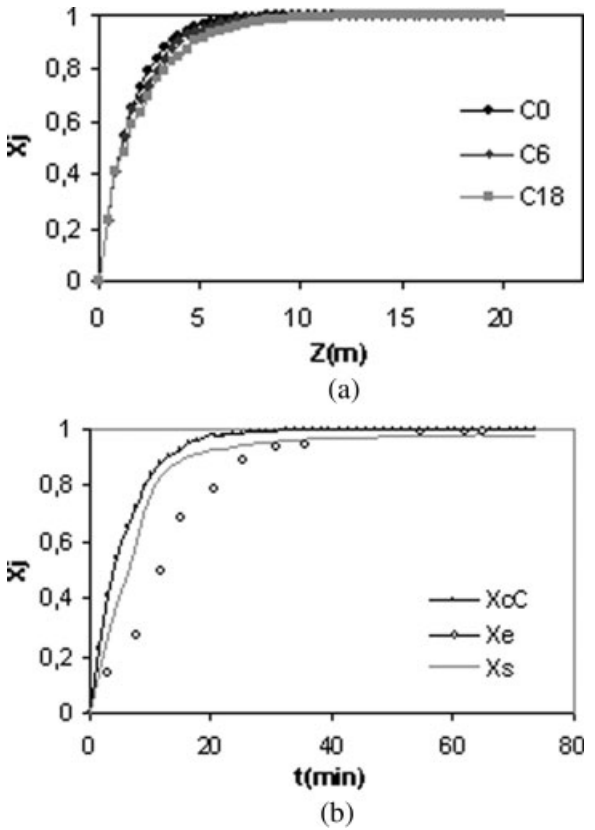

Figure 4 Conversion of monomer (a) without ($N_b = 0$) and with ($N_b = 6$, 18) baffles and (b) experimental validation, both in isothermal conditions, 60°C.

lems. In isothermal condition, the discretization equations, for example eqs. (89), (92), and (95), are linear algebraic equations, and the set of such equations is solved by the methods of linear algebraic equations with the following iterative procedures to find out the value of the number of particle with or without baffle: (1) guess a number of particle, $N_{a,p}$; (2) calculate the initiator and radicals distribution; (3) calculate the number of particle, N_p; (4) compare the N_p with the actual number of particle, $N_{a,p}$; (5) if the absolute value of $|N_p - N_{a,p}|$ is greater than a factor of convergence, then set $N_{a,p} = N_p$ (return to the Step 1). The flow diagram is shown in the Figure 3.

RESULTS AND DISCUSSION

The simulation results of *conversion* (X_j) versus length of the reactor (Z) for styrene without baffle (C0) and with baffles (C6, C18) in isothermal condition (C) at 60°C are displayed in Figure 4(a). The conversion without baffles are higher than the conversion with $N_b = 6$ and 18 baffles. When the baffle number is increased, the conversion exhibits a small decrease due to variation of plug flow condition.

The comparative results, in isothermal condition at 60°C, of computational (X_{cC}), experimental (X_e), and simulation conversion (X_s) (literature results) versus residence time (t) inside TR are shown in Figure 4(b). It can be seen that the experimental and computational conversion has equal properties, but the simulation conversion with a different mathematical model. The experimental and simulation conversions obtained by Bataile[11] were considered. It can be observed that the three curves have the same behavior and validate the numerical method of finite volume through the comparison of experimental and simulation results in isothermal conditions.

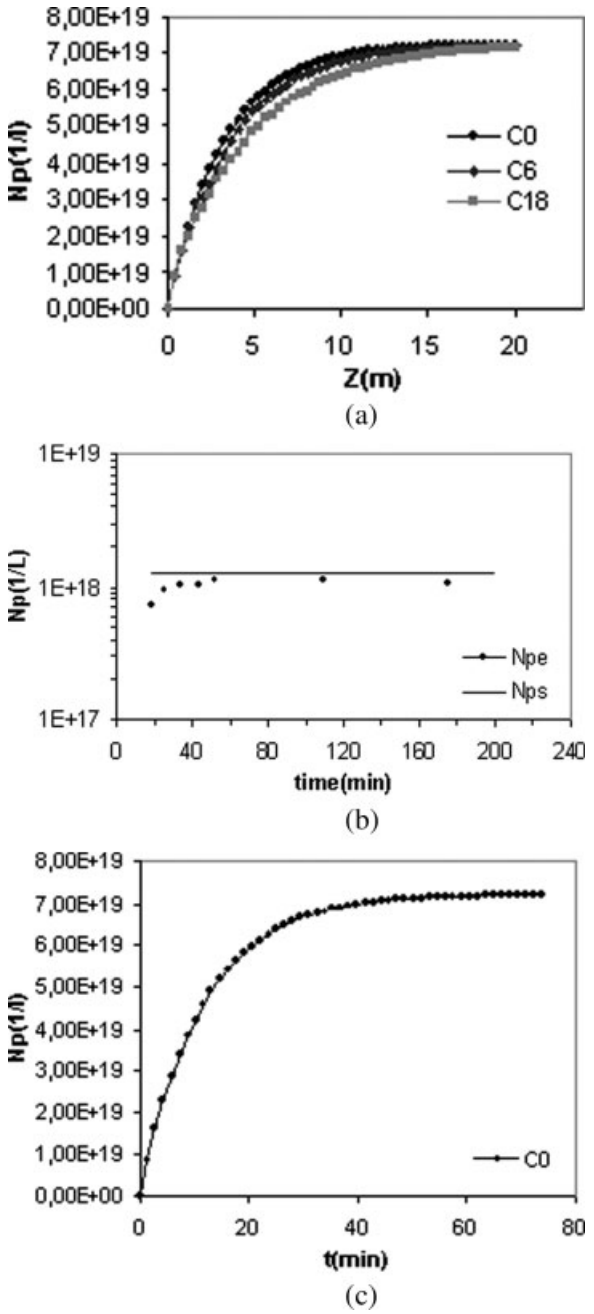

Figure 5 (a) Number of particles with $N_b = 0$, 6, 18 baffles; (b) and (c) validation of number of particles, both in isothermal conditions ($CN_b = 60$°C).

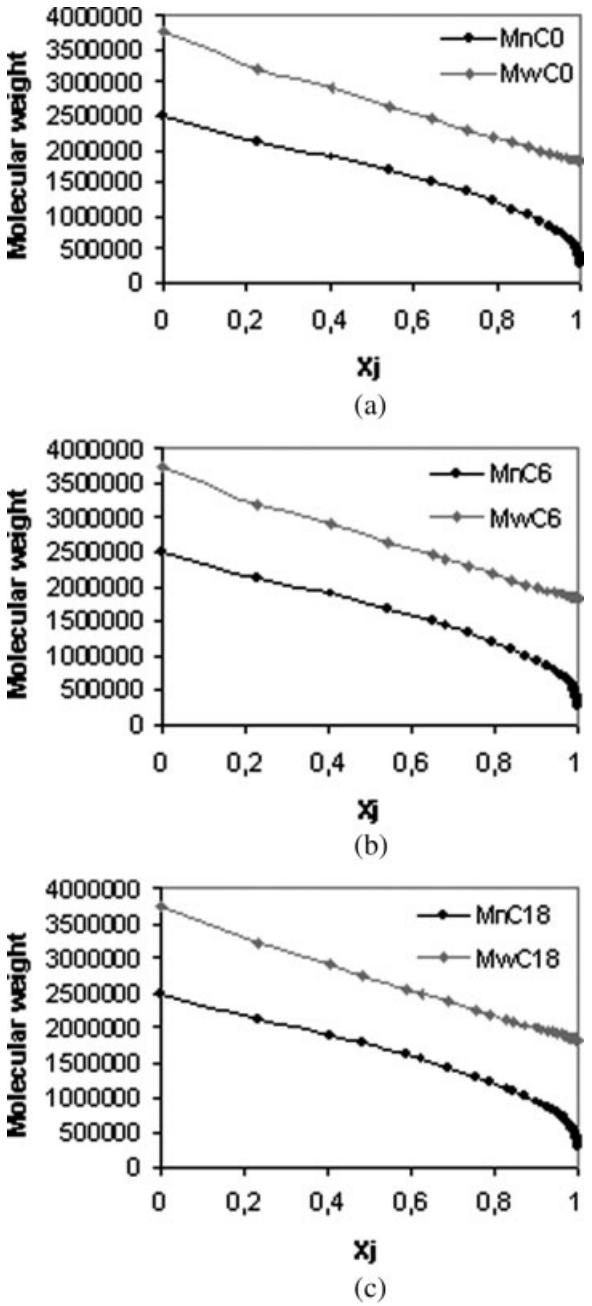

Figure 6 Molecular weight distribution (a) without ($N_b = 0$) and (b) and (c) with ($N_b = 6, 18$) baffles in isothermal ($CN_b = 60°C$) conditions.

The prediction results of the *polystyrene particles number* (N_p) by micellar and homogeneous nucleation mechanism versus length of the reactor (Z) without baffle (C0) and with baffles (C6, C18) in isothermal condition (C) at 60°C are depicted in Figure 5(a). The three curves have the same behavior and show, in isothermal condition, that when the number of baffles increases, the number of particles slightly decreases.

The comparative results, in isothermal condition, of particles' number (N_p) without baffles inside batch and TR, respectively, versus time (t) are presented in Figure 5(b, c). The experimental ($N_{p,e}$) and simulation ($N_{p,s}$) of the particles number is shown in Figure 5(b). The experimental and simulation conditions are a feed temperature of 50°C, 0.011 mol KPS/L, 0.05 mol SDS/L, and no adiabatic process. Bataile et al.[11] indicated, in relation to Figure 5(b), that the experimental results are in a close range within experimental measurement error. and considering the difficulty associated with particle number measurement determination, the model prediction should be considered satisfactory. The particle number for the model prediction is approximately at 1.28×10^{18} L^{-1}, as shown in Figure 5(b). Figure 5(c) presents the prediction of particle number in isothermal condition without baffles inside TR. The particle number varies between 0 and 7.22×10^{19} L^{-1}. The experimental data, as shown in Figure 5(b), present the same performance as that of the simulation shown in Figure 5(c), and the comparison of the two figures allows to conclude that mathematical model and numerical method of FVM were able to represent the system well.

The simulation results of the cumulative average *molecular weight distribution* versus conversion of monomer (X_j), without baffle (M_nC0, M_wC0) and with

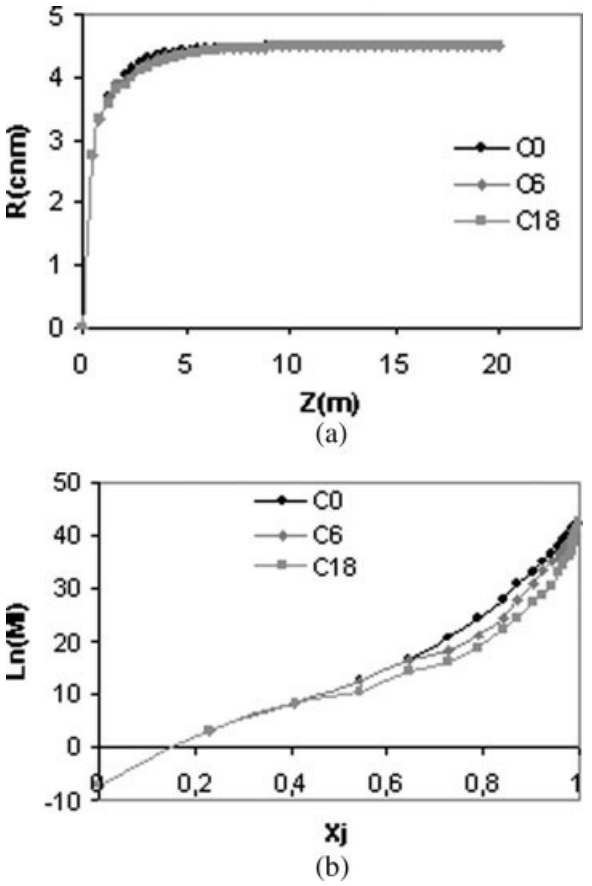

Figure 7 (a) Average particle size distribution and (b) viscosity distribution, both with $N_b = 0, 6, 18$ baffles in isothermal ($CN_b = 60°C$) conditions.

baffles (M_nC6, M_wC6; M_nC18, M_wC18) in isothermal condition at 60°C are shown in Figure 6. Figure 6(a–c) shows that the average molecular weights are different. The number–average (M_n) and weight–average (M_w) molecular weight have a better distribution only marginally when the baffles number increases inside TR.

These comparative results of simulation of the *polystyrene particles size* of unswollen particle radius (R) versus length of the reactor (Z) without baffle (C0) and with baffles (C6, C18) in isothermal condition (C) at 60°C are shown in Figure 7(a). The three curves have the same behavior, but when the baffle number increases, the particle size slightly diminishes.

The predictions results of *polymer viscosity distribution* (ln(μ) inside TR versus conversion of monomer (X_j) without baffle (C0) and with baffles (C6, C18) in isothermal condition (C) at 60°C are given in Figure 7(b). The three curves have similar behavior; the points on path of the curves C0, C6, and C18 show uniform distribution, and when the baffle number increases the viscosity diminishes and varies between $\ln(\mu) = -6.998$ and 42.50. The mathematical model of eq. (24) was used to estimate the viscosity of the three curves.[20]

CONCLUSIONS

In this work an alternative reactor design is proposed. It consists of the placement of baffles inside the tube. This new configuration was compared with empty TR in isothermal conditions. The results show that better polymer properties are obtained when the proposed design is used. The results with baffles were better than without baffles in relation to the desired properties such as particle size and viscosity. It was seen that the problem is sufficiently solved by finite volume method. The simulation results were compared with experimental data (when available for empty tube) and good agreements were obtained.

References

1. Mendoza Marín, F. L.; Ferrareso Lona, L. M.; Wolf Maciel, M. R.; Maciel Filho, R. J Appl Polym Sci 2006, 100, 2572.
2. Paquet, D. A.; Ray, W. H. AIChE J 1994, 40, 88.
3. Chern, C. S. J Appl Polym Sci 1995, 56, 221.
4. Gilbert, R. G.; Emulsion Polymerization—A Mechanistic Approach; Academic Press: London, 1995.
5. Scholtens, C. A. Thesis. Process Development for Continuous Emulsion Copolymerization; CIP-DATA Library Technische Universiteit Eindhoven, Ter Verkrijging van de graad van Doctor, 2002.
6. Bockhorn, H. ULLMANN 'S Encyclopedia of Industrial Chemistry, Vol. B1: Mathematical Modeling; 1992; p 2.
7. Gao, J.; Penlidis, A. Prog Polym Sci 2002, 27, 403.
8. Maciel Filho, R.; Domingues, A. Presented at the Twelfth International Symposium on Chemical Reaction Engineering, ISCRE 12, Turin, Italy, 1992.
9. Kiparissides, C. Chem Eng Sci 1996, 51, 1637.
10. Toledo, E. C. V. Ph.D Dissertation, FEQ/UNICAMP, Campinas, 1999.
11. Bataile, P.; Van, B. T.; Pham, Q. B. J Polym Sci Polym Chem Ed 1982, 20, 795.
12. Mendoza Marín, F. L. Ph.D. Dissertation, FEQ/UNICAMP, Campinas, 2004.
13. Froment, G. F.; Bischoff, K. B. Chemical Reactor Analysis and Design, 2nd ed.; Wiley: New York, 1990.
14. Tucker, C. L., III. Fundamentals of Computer Modeling for Polymer Processing; Hanser: Munich, Germany, 1989.
15. Versteeg, H. K.; Malalasekera, W. An Introduction to Computational Fluid Dynamics—The Finite Volume Method, 2nd ed.; Addison Wesley Longman: Harlow, UK, 1998.
16. Paquet, D. A.; Ray, W. H. AIChE J 1994, 40, 73.
17. Harkness, M. R. M.S. Thesis, Rensselaer Polytechnic Institute, Troy, New York, 1982.
18. Patankar, S. V. Numerical Heat Transfer and Fluid Flow; Hemisphere: New York, 1980.
19. Wendt, J. F. Computational Fluid Dynamics; Springer-Verlag: New York, 1992.
20. Chen, C. C.; Nauman, E. B. Chem Eng Sci 1989, 44, 179.